Transverse charge and magnetization densities in holographic QCD

Dipankar Chakrabarti and Chandan Mondal

Department of Physics, Indian Institute of Technology Kanpur, Kanpur 208016, India

(Dated: February 21, 2014)

arXiv:1402.4972v1 [hep-ph] 20 Feb 2014

Abstract

We present a study of flavor structures of nucleons transverse charge and anomalous magnetization densities for both unpolarized and transversely polarized nucleons. We consider two different models for the electromagnetic form factors in holographic QCD. The flavor form factors are obtained by decomposing the Dirac and Pauli form factors for nucleons using the charge and isospin symmetry. The results are compared with two standard phenomenological parametrizations.

PACS numbers: 13.40.Gp, 11.25.Tq, 12.38.Aw

I. INTRODUCTION

Form factors of the nucleons provide us the crucial informations about the internal structure of the nucleons and have been measured in many experiments. The charge and magnetization densities in the transverse plane are defined as the Fourier transforms of the electromagnetic form factors. The transverse densities are also intimately related to the generalized parton distributions (GPDs) with zero skewness. The contributions of individual quark to the nucleon charge and magnetization densities are obtained from the flavor decompositions of the transverse densities. The transverse densities corresponding to individual quarks are given by the Fourier transforms of the GPDs in the transverse coordinate or impact parameter space[1]. The form factor involves initial and final states with different momentum and three dimensional Fourier transforms cannot be interpreted as densities whereas the transverse densities defined in the infinite momentum frame are free from this difficulty and have proper density interpretation [2–4].

Recently, AdS/QCD has emerged as one of the most promising techniques to unravel the structure of mesons and nucleons. The AdS/CFT conjecture[5] relates a gravity theory in AdS_{d+1} to a conformal theory at the d dimensional boundary. There are many applications of AdS/CFT to investigate the QCD phenomena[6, 7]. A boundary condition in the fifth dimension z in AdS_5 breaks the conformal invariance and allows QCD mass scale and confinement. In the hard-wall model, an IR cutoff is set at $z_0 = 1/\Lambda_{QCD}$ while in soft-wall model, a confining potential in z is introduced. There is an exact correspondence between the holographic variable z and the light front transverse variable ζ which measures the separation of the quark and gluonic constituents in the hadron[8, 9]. The AdS/QCD for the baryon has been developed by several groups [8–14]. Though it gives only the semiclassical approximation of QCD, so far this method has been successfully applied to describe many hadron properties e.g., hadron mass spectrum, parton distribution functions, GPDs, meson and nucleon form factors, structure functions etc[12, 15–22]. AdS/QCD wave functions are used to predict the experimental data for ρ meson electroproduction [23]. AdS/QCD has also been successfully applied in the meson sector to predict the branching ratio for decays of $\bar{B}^0$ and $\bar{B}^0_s$ into ρ mesons [24], isospin asymmetry and branching ratio for the $B \to K^*\gamma$ decays [25], transition form factors[26, 27], etc. There are many other applications in the baryon sector e.g., semi-empirical hadronic momentum density distributions in the transverse plane

have been calculated in[28], in [29], the form facfor of spin 3/2 baryons (Δ resonance) and also the transition form factor between Δ and nucleon have been studied, an AdS/QCD model has been proposed to study the baryon spectrum at finite temperature[30] etc.

The flavor decompositions of the nucleon form factors in a light-front quark model with SU(6) spin-flavor symmetry have been studied in detail in [21] and shown to agree with experimental data. It is interesting and instructive to study the transverse densities and their flavor decomposition in holographic QCD. There are two different holographic QCD models for nucleon form factors developed by Abidin and Carlson[12] and Brodsky and Teramond[18]. Here, we present a detailed analysis of the transverse densities in both the models.

A model-independent transverse charge densities for nucleons in infinite-momentum-frame have been studied in [31] whereas the charge densities in the transverse plane for a transversely polarized nucleon are shown in [32, 33]. In [34], the long range behaviors of the unpolarized quark transverse charge density of the nucleons have been studied. Transverse charge and magnetization densities in the nucleon's chiral periphery(i.e., at a distance $b = \mathcal{O}(1/m_\pi)$) using methods of dispersion analysis and chiral effective field theory has been analysed in [35]. The transverse densities for the quarks are studied in a chiral quark-soliton model in [36]. Using Laguerre-Gaussian expansion, Kelly [37] proposed a parametrization of the nucleon Sachs form factors in terms of charge and magnetization densities. A study of flavor dependence of the transverse densities in a GPD model has been reported in [38]

In [19], the nucleon transverse charge and magnetization densities have been evaluated in the model developed in [12]. In this work, we show that the flavor decompositions of the transverse densities of the nucleons in two different models in the framework of AdS/QCD and compare with the two global parametrizations of Kelly [39] and Bradford *at el* [40]. By decomposing the nucleon form factors F_1 and F_2 using the charge and isospin symmetry, we obtain the flavor form factors F_1^q and F_2^q for the quarks. The Fourier transforms of these electromagnetic form factors give the charge and magnetization densities in the transverse plane.

The paper is organized as follows. A brief description of the the form factors in AdS/QCD has been has given in Sec.II. In Sec.III, the charge and magnetization densities for both unpolarized and transversely polarized nucleons have been studied. The individual flavor contributions are also studied in this section. Then we provide a brief summary in Sec.IV.

II. NUCLEON AND FLAVOR FORM FACTORS IN ADS/QCD

Here we consider the soft wall model of AdS/QCD, where in place of a sharp cutoff z, one introduces a potential. The action in soft model is written as[18]

$$S = \int d^4x dz \sqrt{g} \Big(\frac{i}{2} \bar{\Psi} e_A^M \Gamma^A D_M \Psi - \frac{i}{2} (D_M \bar{\Psi}) e_A^M \Gamma^A \Psi - \mu \bar{\Psi} \Psi - V(z) \bar{\Psi} \Psi \Big), \tag{1}$$

where $e_A^M = (z/R)\delta_A^M$ is the inverse vielbein and $V(z)$ is the confining potential which breaks the conformal invariance and R is the AdS radius.

The Dirac equation in AdS derived from the above action is given by

$$i\Big(z\eta^{MN}\Gamma_M \partial_N + \frac{d}{2}\Gamma_z \Big)\Psi - \mu R \Psi - R V(z) \Psi = 0. \tag{2}$$

With z identified as the light front transverse impact variable ζ which gives the separation of the quark and gluonic constituents in the hadron, it is possible to extract the light-front wave functions for the hadron. In $d = 4$ dimensions, $\Gamma_A = \{\gamma_\mu, -i\gamma_5\}$. To map with the light front wave equation, we identify $z \to \zeta$, where ζ is the light front transverse variable, and substitute $\Psi(x, \zeta) = e^{-iP\cdot x}\zeta^2 \psi(\zeta) u(P)$ in Eq.(2) and set $\mid \mu R \mid = \nu + 1/2$ where ν is related with the orbital angular momentum by $\nu = L + 1$. For linear confining potential $U(\zeta) = (R/\zeta)V(\zeta) = \kappa^2\zeta$, we get the light front wave equation for the baryon in 2×2 spinor representation as

$$\Big(-\frac{d^2}{d\zeta^2} - \frac{1 - 4\nu^2}{4\zeta^2} + \kappa^4\zeta^2 + 2(\nu + 1)\kappa^2 \Big)\psi_+(\zeta) \;=\; \mathcal{M}^2 \psi_+(\zeta), \tag{3}$$

$$\Big(-\frac{d^2}{d\zeta^2} - \frac{1 - 4(\nu + 1)^2}{4\zeta^2} + \kappa^4\zeta^2 + 2\nu\kappa^2 \Big)\psi_-(\zeta) \;=\; \mathcal{M}^2 \psi_-(\zeta). \tag{4}$$

In case of mesons, the similar potential $\kappa^4\zeta^2$ appears in the Klein-Gordon equation which can be generated by introducing a dilaton background $\phi = e^{\pm\kappa^2 z^2}$ in the AdS space which breaks the conformal invariance. But in case of baryon, the dilaton can be scaled out by a field redefinition[18]. So, the confining potential for baryons cannot be produced by dilaton and is put in by hand in the soft wall model. The form of the confining potential $(\kappa^4\zeta^2)$ is unique for both the meson and baryon sectors [41]. The twist-3 nucleon wave functions in the soft wall model are obtained as

$$\psi_+(z) \;=\; \frac{\sqrt{2}\kappa^2}{R^2} z^{7/2} e^{-\kappa^2 z^2/2}, \tag{5}$$

$$\psi_-(z) \;=\; \frac{\kappa^3}{R^2} z^{9/2} e^{-\kappa^2 z^2/2}. \tag{6}$$

Model-I

The SU(6) spin-flavor symmetric quark model is constructed in the AdS/QCD by weighing the different Fock-state component by the charges and spin projections of the partons as dictated by the symmetry. In the light-front quark model the Dirac and Pauli form factors are described by the spin-nonflip and spin-flip matrix elements of the electromagnetic current J^+. The Dirac and Pauli form factors for the nucleons are obtained in this model as

$$F_1^p(Q^2) = R^4 \int \frac{dz}{z^4} V(Q^2, z)\psi_+^2(z), \tag{7}$$

$$F_1^n(Q^2) = -\frac{1}{3} R^4 \int \frac{dz}{z^4} V(q^2, z)(\psi_+^2(z) - \psi_-^2(z)), \tag{8}$$

$$F_2^{p/n}(Q^2) = \kappa_{p/n} R^4 \int \frac{dz}{z^4} V(Q^2, z)\psi_-^2(z). \tag{9}$$

The form factors are normalized to $F_1^p(0) = 1, F_1^n(0) = 0$ and $F_2^{p/n}(0) = \kappa_{p/n}$, the anomalous magnetic moments for the nucleons. The bulk-to-boundary propagator for soft wall model is given by

$$V(Q^2, z) = \Gamma(1 + \frac{Q^2}{4\kappa^2}) U(\frac{Q^2}{4\kappa^2}, 0, \kappa^2 z^2), \tag{10}$$

where $U(a, b, z)$ is the Tricomi confluent hypergeometric function. The bulk-to-boundary propagator, Eq. (10), can be written in a simple integral form [18, 42]

$$V(Q^2, z) = \kappa^2 z^2 \int_0^1 \frac{dx}{(1-x)^2} x^{Q^2/(4\kappa^2)} e^{-\kappa^2 z^2 x/(1-x)}. \tag{11}$$

We refer the formulae for the form factors given in Eqs.(7,8 and 9) as Model-I. It has been shown[20, 21] that the form factors for the nucleons agree with experimental data for $\kappa = 0.4066\ GeV$.

Model-II

The other model of the form factors was formulated by Abidin and Carlson[12]. Since the action defined in Eq.(1) cannot produce the spin flip (Pauli) form factors, they introduced an additional gauge invariant non-minimal coupling. This additional term also gives an anomalous contribution to the Dirac form factor. In this model the form factors are given by[12]

$$F_1^p(Q^2) = C_1(Q^2) + \eta_p C_2(Q^2), \tag{12}$$

$$F_1^n(Q^2) = \eta_n C_2(Q^2), \tag{13}$$

$$F_2^p(Q^2) = \eta_p C_3(Q^2), \tag{14}$$

$$F_2^n(Q^2) = \eta_n C_3(Q^2). \tag{15}$$

where

$$C_1(Q^2) = \frac{a+6}{(a+1)(a+2)(a+3)}, \tag{16}$$

$$C_2(Q^2) = \frac{2a(2a-1)}{(a+1)(a+2)(a+3)(a+4)}, \tag{17}$$

$$C_3(Q^2) = \frac{48}{(a+1)(a+2)(a+3)}, \tag{18}$$

where $a = Q^2/(4\kappa^2)$. The value of κ is fixed by simultaneous fit to proton and rho meson mass and the best fit gives the value $\kappa = 0.350GeV$. The other parameters are determined from the normalization conditions of the Pauli form factor at $Q^2 = 0$ and are given by $\eta_p = 0.224$ and $\eta_n = -0.239$ [12]. We refer the form factors given by Eqs. (12-15) as Model-II.

The Pauli form factors in these two models are identical, the main difference is in the Dirac form factor. In model-II, there is an additional contribution to the Dirac form factor from the non-minimal coupling term. It should be mentioned here that the Pauli form factors in the AdS/QCD models are mainly of phenomenological origin. In Model-I, Dirac and Pauli form factors in light front are identified as the spin-nonflip and spin-flip matrix elements of J^+ current[43]. In Model-II, a non-minimal coupling term is added to generate the Pauli form factors. This additional term gives contribution to the Dirac form factors also. While in the Model-I, the non-minimal coupling term is used to derive the formula for the Pauli form factors in AdS space, but there is no anomalous contribution to the Dirac form factors as the form factors are constructed within SU(6) quark model.

Under the charge and isospin symmetry it is straightforward to write down the flavor decompositions of the nucleon form factors as

$$F_i^u = 2F_i^p + F_i^n \quad \text{and} \quad F_i^d = F_i^p + 2F_i^n, \quad (i = 1, 2) \tag{19}$$

with the normalizations $F_1^u(0) = 2, F_2^u(0) = \kappa_u$ and $F_1^d(0) = 1, F_2^d(0) = \kappa_d$ where the anomalous magnetic moments for the up and down quarks are $\kappa_u = 2\kappa_p + \kappa_n = 1.673$ and $\kappa_d = \kappa_p + 2\kappa_n = -2.033$. It was shown in [44] that though the ratio of Pauli and Dirac form factors for the proton $F_2^p/F_1^p \propto 1/Q^2$, the Q^2 dependence is almost constant for the ratio of the quark form factors F_2/F_1 for both u and d.

III. TRANSVERSE CHARGE AND MAGNETIZATION DENSITIES

The transverse charge density inside the nucleons is given by

$$\rho_{ch}(b) = \int \frac{d^2q_\perp}{(2\pi)^2} F_1(q^2) e^{iq_\perp . b_\perp} = \int_0^\infty \frac{dQ}{2\pi} Q J_0(Qb) F_1(Q^2), \tag{20}$$

where b represents the impact parameter and J_0 is the cylindrical Bessel function of order zero. Similar formula for charge density for flavor $\rho^q_{fch}(b)$ can be written with F_1 is replaced by F_1^q . One can define the magnetization density in the similar fashion to have the formula

$$\widetilde{\rho}_M(b) = \int \frac{d^2q_\perp}{(2\pi)^2} F_2(q^2) e^{iq_\perp . b_\perp} = \int_0^\infty \frac{dQ}{2\pi} Q J_0(Qb) F_2(Q^2), \tag{21}$$

Whereas,

$$\rho_m(b) = -b\frac{\partial \widetilde{\rho}_M(b)}{\partial b} = b\int_0^\infty \frac{dQ}{2\pi} Q^2 J_1(Qb) F_2(Q^2), \tag{22}$$

has the interpretation of anomalous magnetization density [3]. Since these quantities are not directly measured in experiments, actual experimental data are not available. In [4], an approximate estimation of the proton charge and magnetization densities has been done from experimental form factor data. To get an insight into the contributions of the different quark flavors, we evaluate the charge and anomalous magnetization densities for the up and down quarks.

We can define the decompositions of the transverse charge and magnetization densities for nucleons in the similar way as electromagnetic form factors [44]. The charge densities decompositions in terms of two flavors can be written as

$$\begin{aligned} \rho^p_{ch} &= e_u \rho^u_{fch} + e_d \rho^d_{fch}, \\ \rho^n_{ch} &= e_u \rho^d_{fch} + e_d \rho^u_{fch}, \end{aligned} \tag{23}$$

where e_u and e_d are charge of u and d quarks respectively. We should remember that due to the charge and isospin symmetry the u, d quark densities in the proton are the same as the d, u densities in the neutron as shown in [31]

$$\begin{aligned} \rho^u_{ch}(b) &= \rho^p_{ch} + \frac{\rho^n_{ch}}{2} = \frac{\rho^u_{fch}}{2}, \\ \rho^d_{ch}(b) &= \rho^p_{ch} + 2\rho^n_{ch} = \rho^d_{fch}, \end{aligned} \tag{24}$$

where $\rho^q_{ch}(b)$ is the charge density of each quark and ρ^q_{fch} is the charge density for each

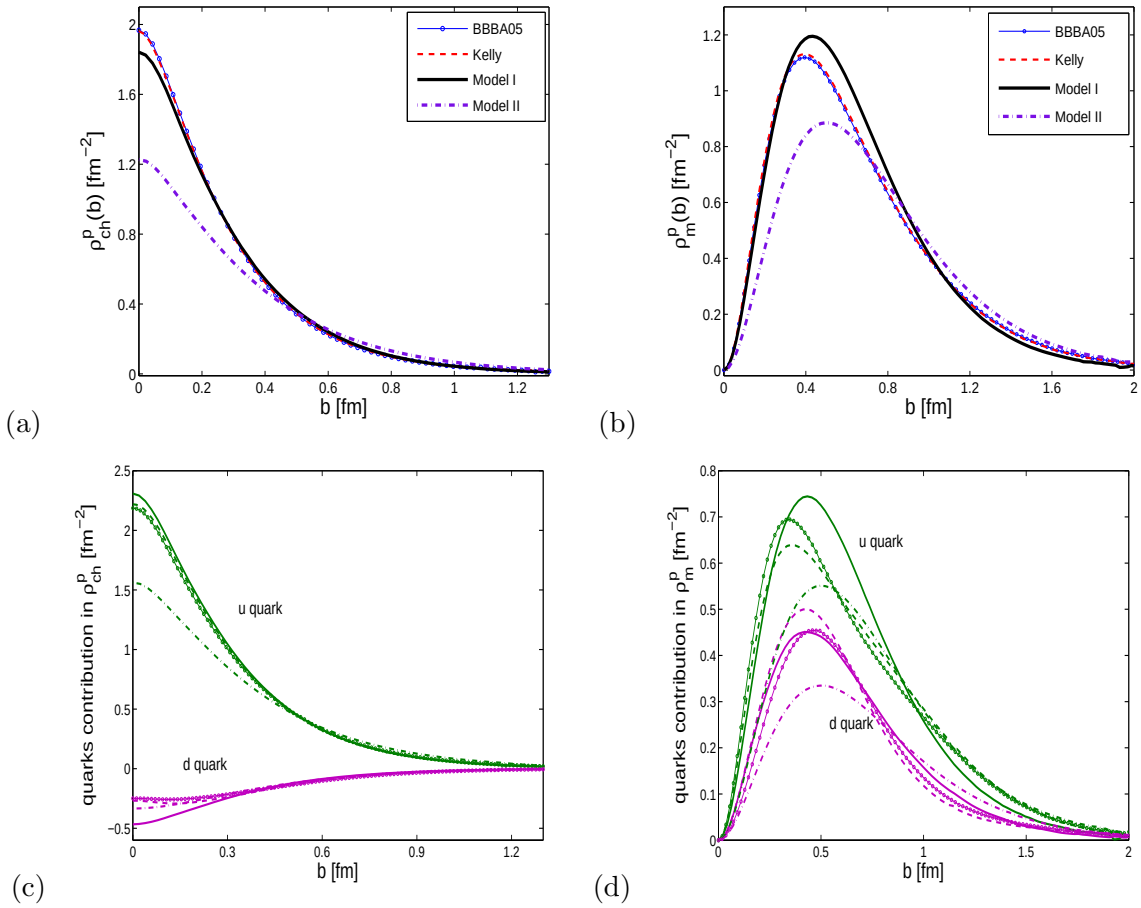

FIG. 1: (Color online) Plots of flavor dependent transverse charge and anomalous magnetization densities for proton. (a) and (b) represent ρ_{ch} and ρ_m for the proton. (c) and (d) represent the contributions from different flavors. Dashed line represents the parametrization of Kelly [39], and the line with circles represents the parametrization of Bradford *at el* [40]; the solid line is for Model-I and dot-dashed line is for Model-II. In (c) and (d) u and d quark contributions are plotted in different colors.

flavor. We can also do the similar decompositions as Eq.(23) and Eq.(24) for ρ_m.

In Fig.1(a) and (b) we show the charge and anomalous magnetization densities for proton. The plots suggest that the Model-I agrees with the phenomenological parametrizations much better than the Model-II. The flavors contributions coming to proton densities from $e_{u/d}\rho^{u/d}_{fch}$ and $e_{u/d}\rho^{u/d}_{fm}$ are shown in Fig.1(c) and (d). Similarly the charge and anomalous magnetization densities for neutron and the flavors contributions $e_{d/u}\rho^{u/d}_{fch}$ and $e_{d/u}\rho^{u/d}_{fm}$ are shown in Fig.2. At small b both the holographic models fail to reproduce the the neutron charge density. Model-I reproduces the neutron magnetization density while model-II again

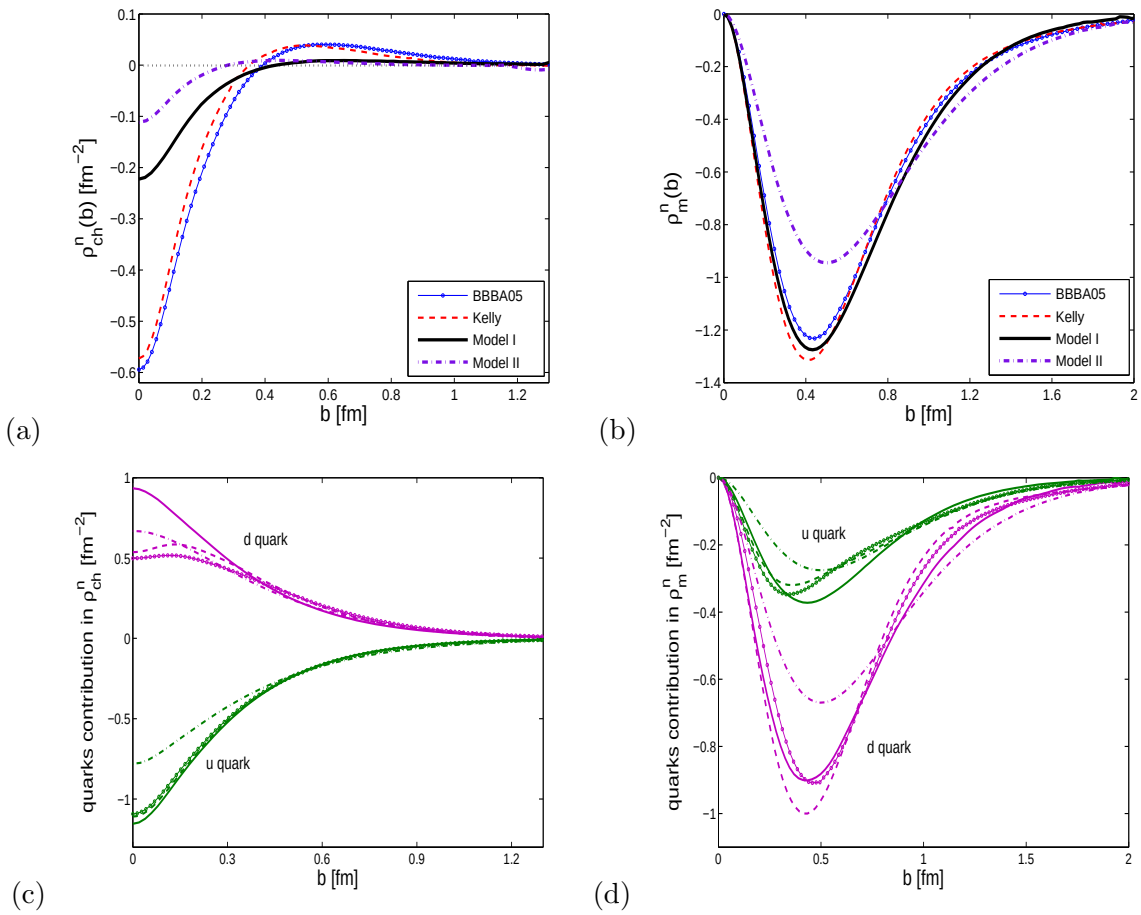

FIG. 2: (Color online) Plots of flavor dependent transverse charge and anomalous magnetization densities for neutron. (a) and (b) represent ρ_{ch} and ρ_m for the neutron. (c) and (d) represent the contributions from different flavors. Dashed line represents the parametrization of Kelly [39], and the line with circles represents the parametrization of Bradford *at el* [40]; the solid line is for Model-I and dot-dashed line is for Model-II. In (c) and (d) u and d quark contributions are plotted in different colors.

fails to agree as shown in Fig.2(b). Model-I results for the u quark contributions to the charge density for both proton and neutron are in excellent agreement with the two different global parametrizations Kelly [39] and Bradford *at el* [40]. The d quark contributions deviate form these two fits. It is not very surprising as it has been already shown[21] for Model-I that the Dirac form factor for d quark itself does not agree well with the experiment results. In case of anomalous magnetization both the quarks contributions in proton and neutron agree quite well with the fits. The charge density for neutron (Fig.2(a)) shows a negatively charged core surrounded by a ring of positive charge density (note that $b = 0$

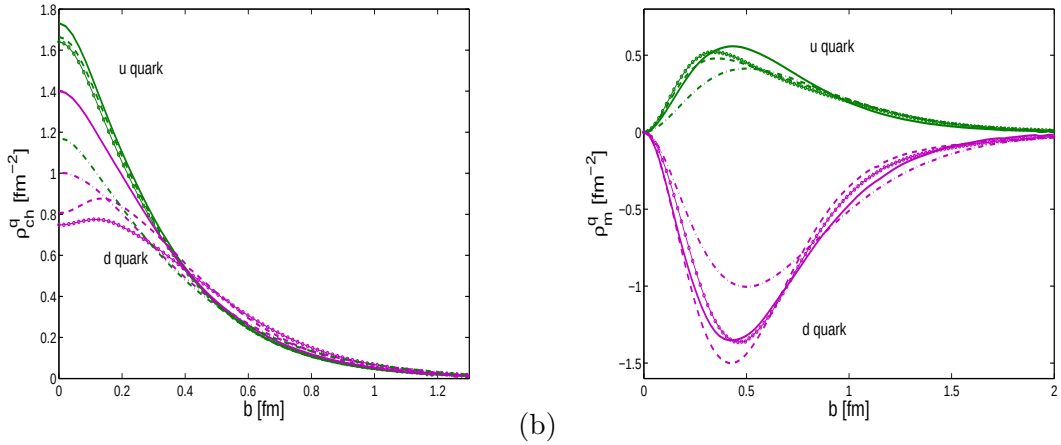

(a) (b)

FIG. 3: (Color online) Plots of quarks transverse charge and anomalous magnetization densities. (a) represent ρ^q_{ch} and (b) represent ρ^q_m. Dashed line represents the parametrization of Kelly [39], and line with circles represents the parametrization of Bradford *at el* [40]; the solid line is for Model-I and dot-dashed line is for Model-II. Densities for u and d quark are plotted in different colors.

corresponds to the centre of the nucleon). In proton charge density the contribution of up quark is large enough compare to down quark but for neutron both contributions from u and d quark are comparable. For anomalous magnetization density of neutron, the d quark contribution is quite high compared to u quark. In Fig. 3 (a) and (b) we show the individual quark's charge and anomalous magnetization densities. The charge density for d quark in Model-I deviates form the fits but is in excellent agreement for u quark. But again, as said before, deviation for d-quark in Model-I is expected. The anomalous magnetization densities in both u and d quarks in Model-I match very well with the fits. It is positive for u quark but negative and larger for d quark. Model-II result for anomalous magnetization density of d-quark does not match so well with the phenomenological fits as Model-I.

For transversely polarized nucleon, the charge density is given by[33]

$$\rho_T(b) = \rho_{ch} - \sin(\phi_b - \phi_s)\frac{1}{2Mb}\rho_m, \tag{25}$$

where M is the mass of nucleon and the transverse polarization of the nucleon is given by $S_\perp = (\cos\phi_s\hat{x} + \sin\phi_s\hat{y})$ and the transverse impact parameter $b_\perp = b(\cos\phi_b\hat{x} + \sin\phi_b\hat{y})$. Without loss of generality, the polarization of the nucleon is taken along x-axis ie., $\phi_s = 0$. The second term in Eq.(25), provides the deviation from circular symmetry of the unpolarized charge density[33]. We show the charge densities for the transversely polarized proton

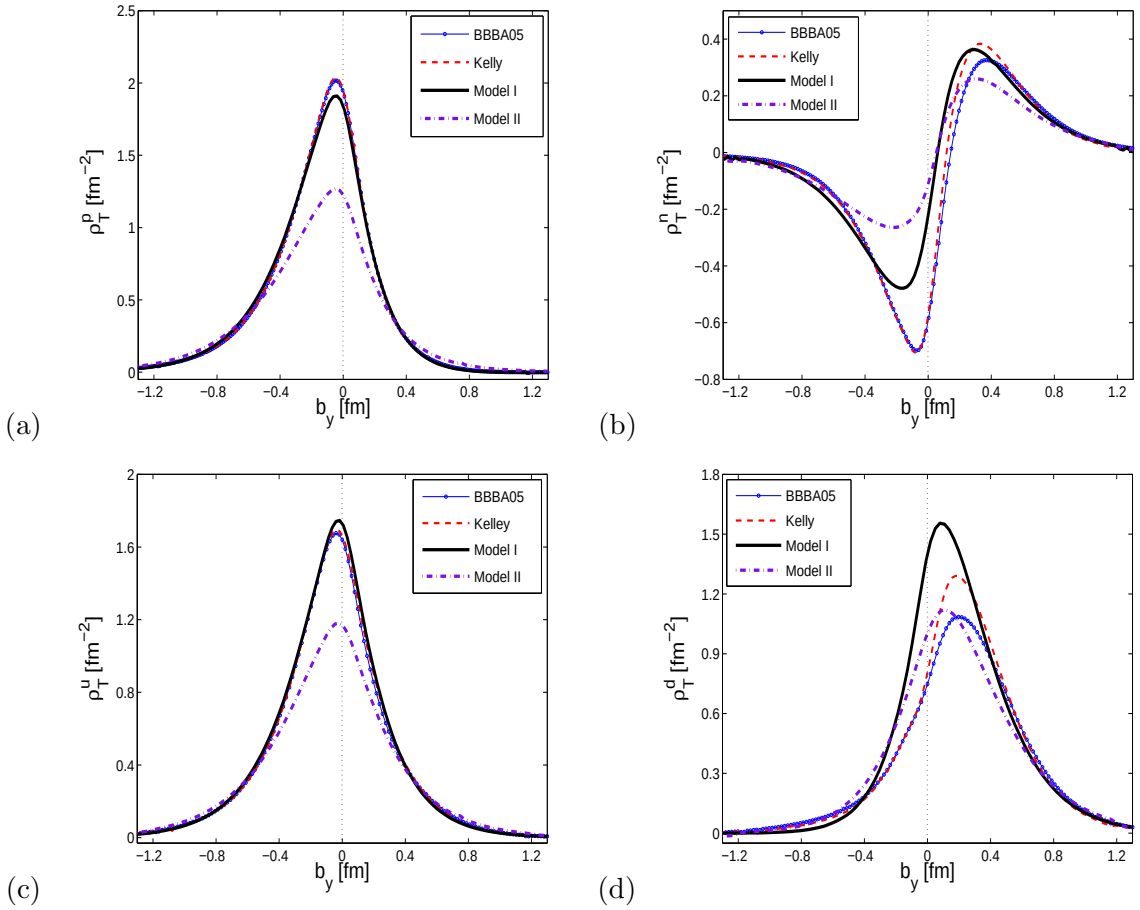

FIG. 4: (Color online) The charge densities for the transversely polarized (a) proton (b) neutron and (c) up (d) down quark charge densities for the transversely polarized nucleon. Dashed line represents the parametrization of Kelly [39], and line with circles represents the parametrization of Bradford *at el* [40]; the solid line is for Model-I and dot-dashed line is for Model-II.

and neutron in Fig.4(a) and 4(b). The u and d quark charge densities for the transversely polarized nucleon are shown in Fig.4(c) and 4(d). Again, in Model-I, the densities for proton and u quark are in good agreement with the global parametrizations but deviate for neutron and d quark. Only for d-quark charge density as shown in Fig.4(d), Model-II agrees with the phenomenological parametrizations better than Model-I. The comparison of charge densities for the transversely polarized and unpolarized proton is shown in Fig.5(a) and the similar plot for neutron is shown in Fig.5(b). For the nucleons polarized along the $+x$ direction,, the charge densities are shifted towards negative b_y direction. The deviation is much larger for the neutron compared to the proton. The behaviors are in agreement with the results reported in [3, 33, 36]. We compare the up and down quark charge densities for the trans-

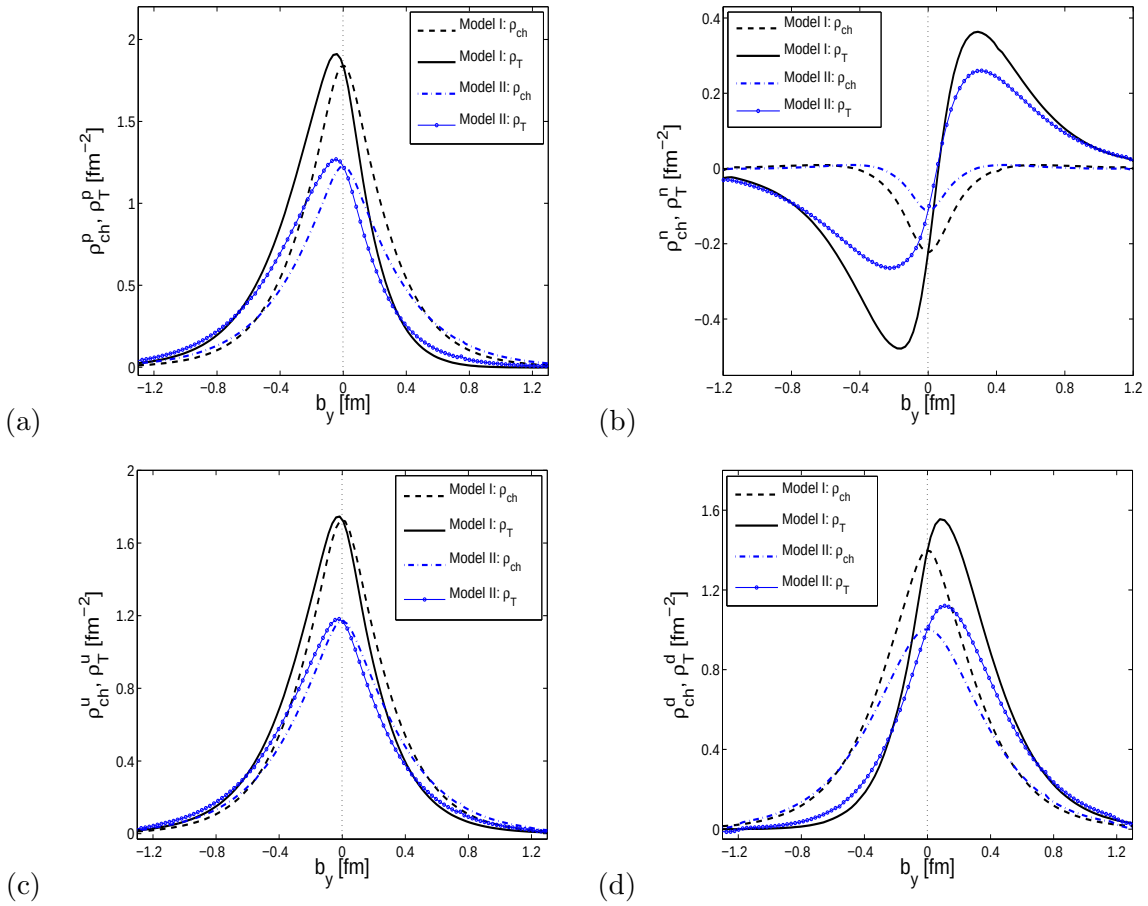

FIG. 5: (Color online) The charge densities for the transversely polarized (a) proton (b) neutron and (c) up (d) down quark charge densities for the transversely polarized nucleon. The unpolarized charge densities are shown by the dashed line.

versely polarized and unpolarized nucleon in Fig.5(c) and 5(d). The deviation or distortion from the symmetric unpolarized density is more for down quark than the up quark. The shifting of charge density for the nucleons polarized in $+x$ direction, is towards positive b_y direction for down quark but opposite for up quark.

IV. SUMMARY

In this paper, we have presented a detailed study and comparison of the charge and anomalous magnetization densities for nucleons in the transverse plane in two models in AdS/QCD. We have also compared our results with the two standard phenomenological parametrizations of the form factors. Both the unpolarized and transversely polarized nucle-

ons have been considered in this work. The unpolarized densities are symmetric in transverse plane while for the transversely polarized nucleons they become distorted. If the nucleon is polarized along x direction, the densities get shifted towards negative y-direction. We have also studied the flavor decompositions of the transverse densities i.e., the charge and anomalous magnetization densities for individual u and d quark flavors. Our analysis shows that Model-I reproduces the data much better than the Model-II. The agreement is not so good for d quark which is consistent with the findings in [21], where the form factors for the d -quark were shown to deviate from the experimental results. For transversely polarized nucleon, the distortion in d quark charge density is found to be stronger than that for u quark and shifted in opposite direction to each other.

Acknowledgments

We thank V.E. Lyubovitskij, S. J. Brodsky and G. F. de Teramond for insightful correspondence on formfactors in AdS/QCD.

---

[1] M. Burkardt, Phys. Rev D. **62**, 071503 (2000), Int. J. Mod. Phys. A **18**, 173 (2003).

[2] G. A. Miller, Phys. Rev. C **80**,045201 (2009).

[3] G. A. Miler, Annu. Rec. Part. Sci. **60**,1 (2010).

[4] S. Venkat, J. Arrington, G. A. Miller and X. Zhan, Phys. Rev. C **83**, 015203 (2011).

[5] J. Maldacena, Adv. Theor. Math. Phys. **2**, 231 (1998).

[6] J. Polchinski and M. J. Strassler, Phys. Rev. Lett. **88**, 031601 (2002); JHEP **0305**, 012 (2003).

[7] L. Cornalba and M. S. Costa, Phys. Rev. D **78**, 096010 (2008); R. C. Brower, M. Djuric, I. Sarcevic and C. -I Tan, JHEP **1011**, 051 (2010); M. S. Costa and M. Djurić, Phys. Rev. D **86**, 016009 (2012);M. S. Costa, M. Djurić and N. Evans, JHEP **1309**, 084 (2013).

[8] S. J. Brodsky and G. F. de Téramond, Phys. Lett. B **582**, 211 (2004).

[9] S. J. Brodsky and G. F. de Téramond, Phys. Rev. Lett. 96, 201601 (2006), Phys. Rev. D 77, 056007 (2006).

[10] J. Erlich, E. Katz, D. T. Son and M. A. Stephanov, Phys. Rev. Lett. **95**, 261602 (2005).

[11] T. Sakai and S. Sugimoto, Prog. Theo. Phys. **113**, 843 (2005).

[12] Z. Abidin and C. E. Carlson, Phys. Rev. D 79, 115003 (2009).

[13] H. Forkel, M. Beyer and T. Frederico, Int. J. Mod. Phys. **E16**, 2794 (2007), W. de Paula, T. Frederico, H. Forkel and M. Beyer, Phys. Rev. **D 79**, 75019 (2009).

[14] A. Vega, I Schmidt, T. Branz, T. Gutsche, V. E. Lyubovitskij, Phys. Rev. **D 80**, 055014 (2009).

[15] Z. Abidin and C. E. Carlson, Phys. Rev. D **77**, 095007 (2008).

[16] S. J. Brodsky and G. F. de Téramond, Phys. Rev. **D 77**, 056007 (2008); Phys. Rev. **D 78**, 025032 (2008).

[17] S. J. Brodsky and G. F. de Téramond, Phys. Rev. **D 83**, 036011(2011), Phys. Rev **D 85**, 096004 (2012).

[18] S. J. Brodsky and G. F. de Téramond, arXiv:1203.4025 [hep-ph].

[19] A. Vega, I. Schimdt, T. Gutsche and V. E. Lyubovitskij, Phys. Rev. D 83, 036001 (2011); Phys. Rev. D 85, 096004 (2012); T. Gutsche, V. E. Lyubovitskij, I. Schmidt and A. Vega, Phys. Rev. **D 86**, 036007 (2012).

[20] D. Chakrabarti and C. Mondal, Phys. Rev. D **88**, 073006 (2013).

[21] D. Chakrabarti and C. Mondal, Eur. Phys. J. C **73**, 2671 (2013).

[22] K. Hashimoto, T. Sakai and S. Sugimoto, Prog. Theor. Phys. **120**, 1093 (2008).

[23] J. R. Forshaw and R. Sandapen, Phys. Rev. Lett. **109**, 081601 (2012).

[24] M. Ahmady and R. Sandapen, Phys. Rev. **D 87**, 054013 (2013).

[25] M. Ahmady and R. Sandapen, Phys. Rev. **D 88**, 014042 (2013).

[26] Z. Abidin and C. E. Carlson, Phys. Rev. **D 80**, 115010 (2009).

[27] M. Ahmady, R. Campbell, S. Lord and R. Sandapen, arXiv:1401.6707 [hep-ph] (2014).

[28] Z. Abidin and C. E. Carlson, Phys. Rev. **D 78**, 071502 (2008).

[29] H. C. Ahn, D. K. Hong, C. Park and S. Siwach, Phys. Rev D. **80**, 054001 (2009).

[30] Z. Li and B. Q. Ma, arXiv:1312.3451 [hep-ph] (2013).

[31] G. A. Miller, Phys. Rev. Lett. **99**, 112001 (2007).

[32] O.V. Selyugin and O.V. Teryaev, Phys. Rev. D**79**, 033003 (2009).

[33] C. E. Carlson and M. Vanderhaeghen, Phys. Rev. Lett. **100**, 032004 (2008).

[34] M. Vanderhaeghen, T. Walcher, arXiv:1008.4225 [hep-ph].

[35] C. Granados, C. Weiss, JHEP **1401**, 092 (2014).

[36] A. Silva, D. Urbano and H. Kim, arXiv:1305.6373 [hep-ph].

[37] J. J. Kelly, Phys. Rev. C **66**, 065203 (2002).

[38] J. O. Gonzalez-Hernandez, S. Liuti, G. R. Goldstein and K. Kathuria, Phys. Rev. C **88**, 065206 (2013).

[39] J. J. Kelly, Phys. Rev. C**70**, 068202 (2004).

[40] R. Bradford, A. Bodek, H. Budd, and J. Arrington Nucl.Phys.Proc.Suppl.**159**,127 (2006).

[41] S. J. Brodsky, G. F. de Téramond, H. G. Dosch, arXiv: 1302.5399 [hep-ph].

[42] H. R. Grigoryan and A. V. Radyushkin, Phys. Rev. D **76**, 095007 (2007).

[43] S. J. Brodsky and S. D. Drell, Phys. rev. D **22**, 2236 (1980).

[44] G. D. Cates, C. W. de Jager, S. Riodian and B. Wojtsekhowski, Phys. Rev. Lett. **106**, 252003 (2011).